



CHEMISTRY

A European Journal



Accepted Article

Title: Superbenzene-Porphyrin Gas-Phase Architectures Derived from Intermolecular Dispersion Interactions

Authors: Dominik Lungerich, Jakob F. Hitzenberger, Frank Hampel, Thomas Drewello, and Norbert Jux

This manuscript has been accepted after peer review and appears as an Accepted Article online prior to editing, proofing, and formal publication of the final Version of Record (VoR). This work is currently citable by using the Digital Object Identifier (DOI) given below. The VoR will be published online in Early View as soon as possible and may be different to this Accepted Article as a result of editing. Readers should obtain the VoR from the journal website shown below when it is published to ensure accuracy of information. The authors are responsible for the content of this Accepted Article.

To be cited as: *Chem. Eur. J.* 10.1002/chem.201803684

Link to VoR: <http://dx.doi.org/10.1002/chem.201803684>

Supported by
ACES

WILEY-VCH

Superbenzene–Porphyrin Gas-Phase Architectures Derived from Intermolecular Dispersion Interactions

Dominik Lungerich,^[a,c] Jakob F. Hitzengerger,^[b] Frank Hampel,^[a] Thomas Drewello^{*,[b]} and Norbert Jux^{*,[a]}

Abstract: A systematic series of superbenzene-porphyrin conjugates was synthesized and characterized. All conjugates show a high degree of cluster formation that correlates to the amount of *t*-butylated hexa-*peri*-hexabenzocoronenes (*t*BuHBCs) attached to the porphyrin's periphery. Determined by mass spectrometry and X-ray diffraction, van der Waals (vdW) interactions like London dispersions (LD), stemming from solubilizing *t*-butyl groups, were identified to be the major reason for the cluster formation. Cluster sizes comprised of more than twenty molecules with masses up to 70.000 Da were observed, which are rare examples of large architectures based on synthetic functional molecules, assembled by dispersion interactions. Novel strategies towards the design of solution processable functional materials, capable of dynamic transformations based on non-covalent synthesis can be envisioned.

Introduction

The impact on the formation of condensed matter by means of dispersion interactions, as it is true for e.g., alkanes, was known since the early explorations by van der Waals (vdW) in the late 19th century and was subsequently recognized by a Nobel prize in 1910.^[1] Nowadays, vdW interactions are the foundation of basic organic chemistry and taught in first-year undergraduate level classes; however, these concepts are often forgotten when it comes to structure design. Bulky substituents like e.g., cyclohexyl, adamantyl or *tert*-butyl (*t*Bu) groups, are often installed under the premise of Pauli repulsion, thus as sterically demanding and potentially solubilizing groups.^[2,3] However, recent theoretical^[4-7] and experimental work^[8-11] led to the rise of so-called dispersion-energy-donors (DEDs). The attractive interactions based on oscillating dipole moments, called London

dispersion (LD),^[12,13] are the foundation of σ - σ interactions in DEDs, as they are true for *tert*-butyl groups. Still, on paper *t*Bu groups appear as bulky substituents and indeed, usually solubilizing effects are mostly observed. However, these nonpolar, though highly polarizable groups were found to be the key for the preparation and intramolecular stabilization of unprecedented and putatively bulky all-*meta-t*-butylated hexaphenylethane through attractive CH-CH (σ - σ) interactions.^[10] Similarly, intermolecular LD interactions were found to be the main driving force for the record holder of the smallest observed H...H bond, which was obtained for all-*meta-t*-butylated triphenylmethane dimers.^[9] Further, precise crystal engineering of *tert*-butylated triptycene derivatives showed also very close *t*Bu-*t*Bu interactions in the solid state.^[14] By means of gas-phase experiments,^[15-18] molecular balance studies,^[8,19-27] and advances in computational methodologies,^[4,28,29] the view on London dispersion clearly changed during the last decade.^[2,30] The scientific community realized how nature is taking advantage of these interactions for the assembly of large architectures.^[6] To our surprise, aside from molecular balance models, experimentally, LD and related vdW interactions were mainly investigated in rather "small" and "innocent" molecules.^[9,10,31-34] However, due to its R^6 -dependency, the true power of LD starts to unfold in large systems with >100 atoms.^[2,35] Nonetheless, the role of dispersion interactions, was proposed to open unprecedented design strategies for innovative supramolecular materials concepts.^[36] These novel perspectives let us re-investigate the possibility of LD interactions in superbenzene-porphyrin conjugates,^[37-40] which we originally started to investigate as graphene-porphyrin hybrid materials for the application in organic electronics. We reviewed our findings from 2014, in which we showed peculiar gas-phase cluster formations of the first bis-HBC-porphyrin conjugate [*trans*HBC]P.^[38] X-ray diffraction analysis (XRDA) of [*trans*HBC]P did not show any intermolecular packing motifs, since *n*-heptane molecules were found to be intercalated between the π -surfaces of the conjugate and thus, acted as "insulator" between the molecules (see figure 1 bottom). On the other hand, XRDA of the respective Zn^{II}-complex [*trans*HBC]PZn,^[38] which was crystallized in the absence of *n*-heptane, showed distinct HBC-HBC interaction in the solid-state, despite the presence of "bulky" *t*Bu-groups in the periphery of the HBC moiety (see figure 1 bottom). Herein, we communicate for the first time our comprehensive and systematic study on the effect of *t*BuHBC units attached to a central porphyrin core. By means of mass spectrometric and X-ray diffraction experiments, dispersion interactions, promoting the formation of radical cation-clusters in the gas phase could be identified. The findings can lead to new design strategies for non-covalent syntheses of larger architectures.[‡]

- [a] Dr. D. Lungerich, Dr. F. Hampel, Prof. Dr. N. Jux
Department of Chemistry and Pharmacy & Interdisciplinary Center for Molecular Materials (ICMM), Organic Chemistry II
Friedrich-Alexander-University Erlangen-Nuernberg
Nikolaus-Fiebiger-Str. 10, 90458 Erlangen, Germany
E-mail: norbert.jux@fau.de
- [b] Dr. J. F. Hitzengerger, Prof. Dr. T. Drewello
Department of Chemistry and Pharmacy, Physical Chemistry I
Friedrich-Alexander-University Erlangen-Nuernberg
Egerlandstr. 3, 90458 Erlangen, Germany
E-mail: thomas.drewello@fau.de
- [c] Dr. D. Lungerich
Department of Chemistry & Molecular Technology Innovation Chair
University of Tokyo
7-3-1 Hongo, Bunkyo-ku, Tokyo 113-0033, Japan

Supporting information for this article is given via a link at the end of the document.

Results and Discussion

We approached our investigations by the preparation of mono-, bis-, tris- and tetra-substituted HBC-porphyrin scaffolds (see figure 1 top and scheme 1), which were synthesized by modified Lindsey-type condensation protocols^[41-44] of formylated hexaphenylbenzene **HPB-CHO** or hexabenzocoronene **HBC-CHO**.^[38] Briefly, in case of conjugates **1-4** (scheme 1 top), a fast microwave-assisted porphyrin condensation method, which allows to work in ten times higher concentrations (100 mM) worked efficiently for **HPB-CHO**.^[43,44] On the other hand, the solubility of **HBC-CHO** revealed to be too low and therefore typical Lindsey conditions at 10 mM concentration had to be carried out.^[41] The outcome of the Scholl oxidation of the hexaphenylbenzene-porphyrin conjugates (**5-7**) could be

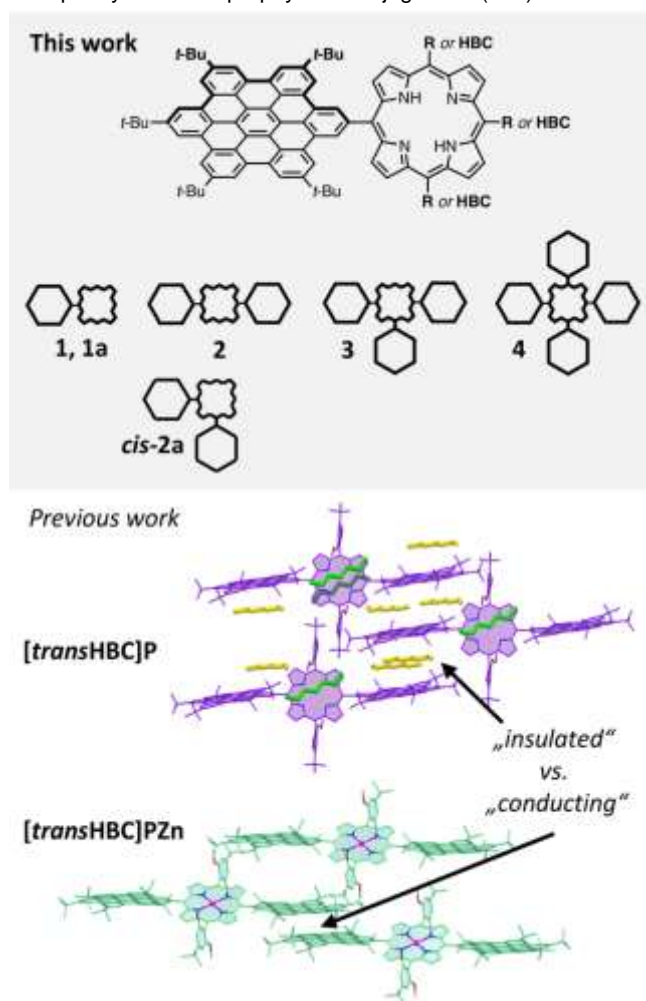
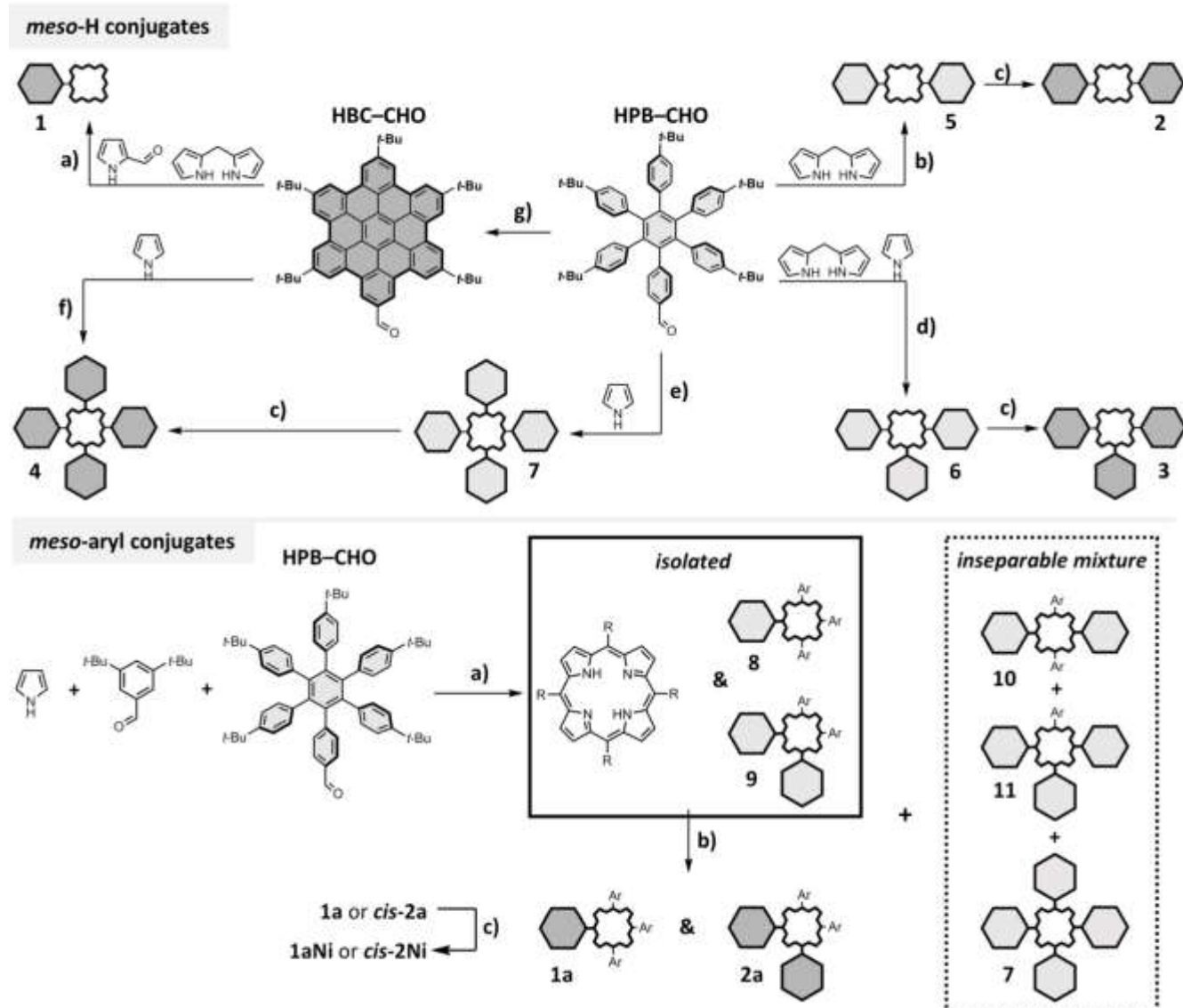


Figure 1. Top: herein investigated superbene-porphyrin scaffolds; R = H for **1**, **2**, **3**; R = 3,5-di-*t*-butylphenyl for **1a** and **cis-2a**; bottom: solid-state packing of **[transHBC]P** with intercalated *n*-heptane molecules indicated in yellow and green; below: solid-state packing of **[transHBC]PZn**.

improved by the addition of small amounts of TFA, because the solubility of the conjugates increased due to the protonation of

the inner nitrogen atoms.^[39] Additionally, possible intermolecular oxidative dimerization reactions at the unsubstituted *meso*-position (in case of **5** and **6**) could be suppressed, since the electron density at the electron-rich *meso*-positions was reduced due to the protonation of the porphyrin core.^[45] Overall one can say that the condensation with **HPB-CHO** followed by Scholl oxidation works more efficiently, than the direct condensation of **HBC-CHO**. However, in case of **1**, a successful isolation could be only achieved starting directly from **HBC-CHO**, because the respective HPB-porphyrin showed incredibly poor solubility and isolation from the other statistical isomers failed.^[42] The higher solubility of **1** compared to its HPB-analogue can be explained by the out-of-plane rotation of the HBC moiety, whereas the respective HPB remains in plane with the porphyrin. The *meso*-aryl (aryl = 3,5-di-*t*-butylphenyl) conjugates were prepared analogously, in a microwave-assisted statistical mixed condensation reaction;^[44] only mono-HPB-porphyrin **8** and *cis*-bis-HPB-porphyrin **9** could be successfully isolated from *trans*-bis-, tris- and tetra-conjugates **10**, **11** and **7**. **8** and **9** were converted to the desired HBC-conjugates **1a** and *cis*-**2a** in a Scholl oxidation reaction under standard conditions. Attempts to separate the mixture of HPB-porphyrin conjugates **10**, **11** and **7** by column chromatography on SiO₂ as well as by size-exclusion chromatography on sephadex SX1 failed. Scholl oxidation of the mixture to the respective HBC-porphyrin mixture, followed by a chromatographic separation remained unsuccessful as well. Ni^{II}-complexes **1aNi**, *cis*-**2aNi** and **4Ni** were obtained from the conversion of the free-base conjugates with Ni(acac)₂ in toluene at 130 °C. Further synthetic details can be extracted from the supporting information.

In order to avoid inherent substituent effects from moieties other than HBCs attached to the porphyrin, the aryl-free, *meso*-H porphyrins were considered first and subjected to matrix-assisted laser desorption/ionization (MALDI) mass spectrometry (MS). DCTB (*trans*-2-[3-(4-*t*Bu-phenyl)-2-methyl-2-propenylidene]malononitrile) was used as matrix and resulted in the formation of HBC-porphyrin radical cations. In order to avoid the detection of concurrent dissociations of metastables,^[46] which would result in the distortion of the cluster distribution, the ions were detected in a time of flight (ToF) detector in linear mode. As a simple criterion for the cluster formation ability, we defined the ratio *D* between the signal intensities of the dimer *I_D* versus the intensity of the monomer *I_M*, $D = I_D/I_M$. A clear correlation between the amount of HBC units and *D* can be identified. As depicted in figure 2a, the mono-HBC-porphyrin conjugate **1** shows a *D* ratio of 8%. *D* further increases to 14% for bis-conjugate **2** and reaches its maximum with 24% for **3** and **4**. Interestingly, while the *D*/HBC seems to average at a value of $8 \pm 1\%$, the fourth HBC unit seems not to have an additional effect on the clustering ability. We attribute this to the spacial coverage of HBCs into all three dimensions already for **3**, and obviously, it does not further improve with four HBCs as in case of **4**.



Scheme 1. Top: Synthesis of *meso*-H substituted HBC-porphyrin conjugates **1–4**: a) CH₂Cl₂, 1 equiv. DPM, 2 equiv. pyrrole-2-carbaldehyde, cat. TFA, rt, 18 h, then DDQ, rt, 1.5 h, (**4** 4%); μ W: CH₂Cl₂, 1 equiv. DPM, cat. I₂, 40 °C, 10 min, then *para*-chloranil, 40 °C, 2 min, (**2** 95%, **3** 93%, **4** 87%); c) CH₂Cl₂, TFA, 16 equiv. FeCl₃/MeNO₂ (per HPB), 0 °C to rt, 18 h, 2 cycles (**2** 95%, **3** 93%, **4** 87%); d) μ W: CH₂Cl₂, 0.33 equiv. DPM, 0.66 equiv. pyrrole, cat. I₂, 40 °C, 10 min, then *para*-chloranil, 40 °C, 2 min, (**6** 9%, **7** 21%); e) μ W: CH₂Cl₂, 1 equiv. pyrrole, cat. I₂, 40 °C, 10 min, then *para*-chloranil, 40 °C, 1 min, (**3** 99%); f) CH₂Cl₂, 1 equiv. pyrrole, cat. BF₃OEt₂, cat. EtOH, rt, 1 h, then DDQ, rt, 1.5 h, (**4** 11%); g) CH₂Cl₂, 16 equiv. FeCl₃/MeNO₂, 0 °C, 3 h, (**8** 88%); Bottom: Statistical synthesis of *meso*-arylated HBC-porphyrin conjugates **1a**, *cis*-**2a** and the nickel complexes **1aNi**, *cis*-**2aNi** and **4Ni**: h) μ W: CH₂Cl₂, 2 equiv. pyrrole, cat. I₂, 40 °C, 5 min, then *para*-chloranil, 40 °C, 1 min (**8** 18%, **9** 24%); i) CH₂Cl₂, TFA, 16 equiv. FeCl₃/MeNO₂ (per HPB), 0 °C to rt, 18 h, (**1a** 99%, *cis*-**2a** 80%); j) μ W: toluene, 20 equiv. Ni(acac)₂, 130 °C, 1 h, (**1aNi** 99%, **2aNi** 99%, **4Ni** 99%); acac = acetylacetonate, DDQ = 2,3-dichloro-5,6-dicyano-1,4-benzoquinone, DPM = dipyrromethene μ W = microwave reactor, TFA = trifluoroacetic acid.

Alteration of the analyte-to-matrix ratio from 1:50 to 1:5000 does not affect the appearance of the mass spectra. Laser desorption/ionization (LDI) on the other hand, gives nothing except monomers of the respective conjugates and thus in-gas-phase cluster formations can be ruled out. It is reasonable to expect that the clusters are pre-formed during the crystallization on the target plate; MALDI then transfers these clusters into the gas phase. The harsh conditions of direct laser irradiation in LDI leads to the complete dissociation of the pre-formed clusters and no evidence could be found that support an in-gas-phase cluster formation. Intermolecular covalent bond formations could be

excluded as well, since the clusters dissociate upon changing from linear to reflectron mode while passing through the spectrometer.^[38] With an increasing I_D/I_M ratio, an inherent increase of cluster sizes can be observed. The largest clusters that were identified for **1** contained up to six molecules, whereas a steady increase for **2** with up to nine molecules, and **3** and **4** with >20 molecules could be detected, hence forming nano-architectures reaching masses way beyond 50.000 Da or 70.000 Da, respectively, (see figure 2b for **4** and figures S1–S4 for **1**, **2** and **3**).

To identify the active part in the cluster formation, observed for the conjugates, we performed electrospray ionization (ESI) of tetraphenylporphyrin (TPP) and hexa-*t*-butyl-HBC (**tBuHBC**), which undergo cluster formations in ESI (compare figure S5). By performing energy-resolved collision-induced dissociation (CID) of the dimer cation from **tBuHBC**, TPP and a mixture of both (TPP/**tBuHBC**) the role of the porphyrin moiety as the active cluster part could be ruled out. As shown in figure 2c, TPP shows only very weak interactions and fragmentation takes place already at low energies. In comparison, the cluster strength increases drastically for the TPP/**tBuHBC** dimer and finds its maximum for the pure **tBuHBC** dimers. However, at that

occupation of higher lying orbitals increases their polarizability and hence, leads to increased dispersion interactions in the cluster material.^[47]

This hypothesis is further supported by the ultrafast energy-transfer from the HBC to the porphyrin upon excitation of the HBC's β -band (compare absorption and emission spectra in figure 5; discussion of the optical spectra can be found at the end of the manuscript).^[37,38] Unfortunately, reliable and high level DFT computations, which include dispersion contributions require large basis sets and electron correlation corrections; common functionals like e.g., B3LYP are inefficient in describing the LD contributions in supramolecular gas-phase assemblies.

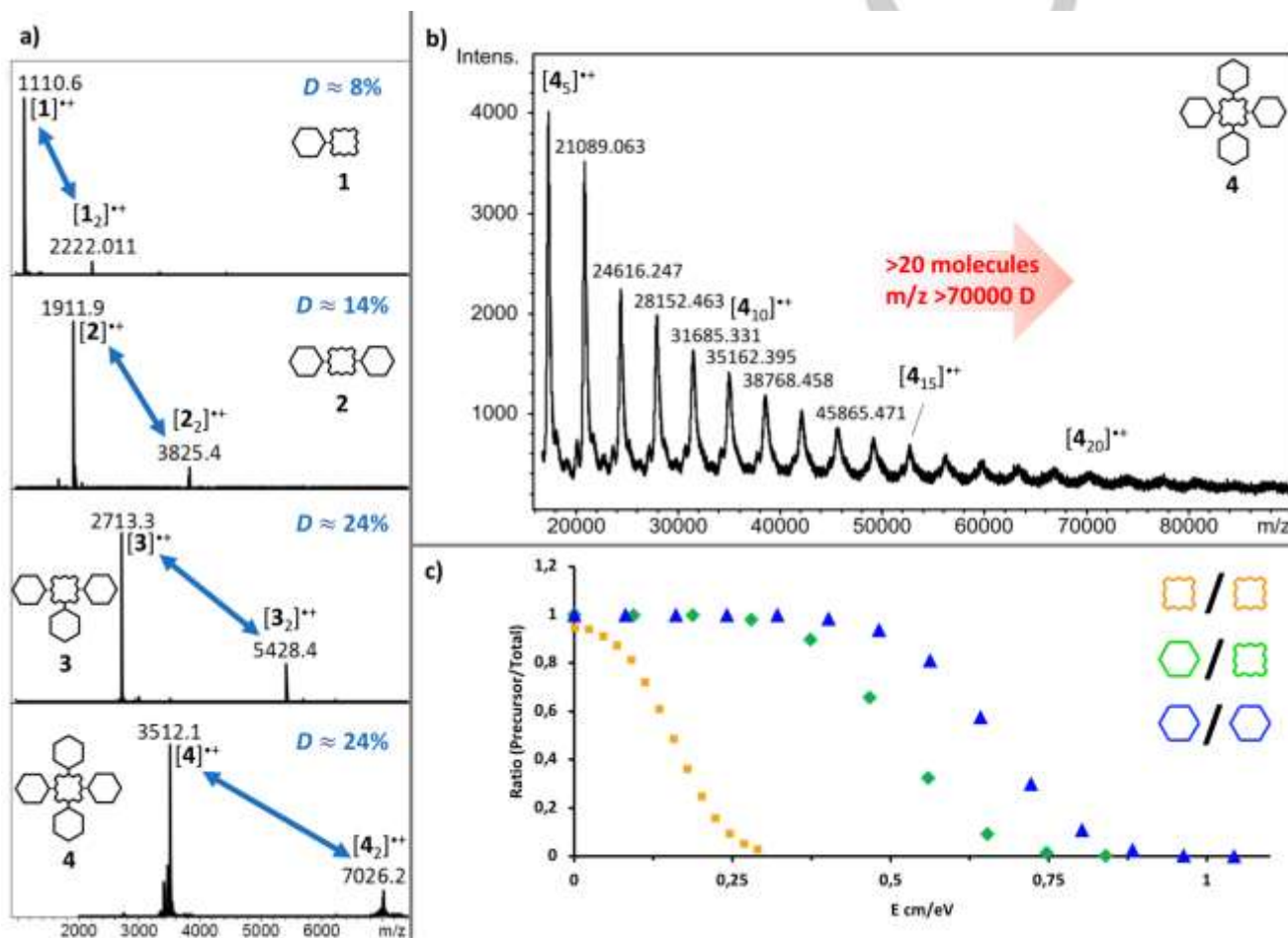


Figure 2. Cluster experiments in MS: a) determination of the cluster ability ratio D by MALDI MS in linear mode; b) zoom-in into the high mass region of [4]_{*n*}ⁿ⁺ clusters; c) relative comparison of energy dependent CID of dimers from TPP (orange), TPP/**tBuHBC** mixture (green) and **tBuHBC** (blue).

point it should be noticed that neither **tBuHBC** clusters nor TPP/**tBuHBC** mixed-clusters are formed during MALDI, and thus, this phenomenon can be solely attributed to the HBC-porphyrin conjugates (compare figure S6–S8). We believe this could be related to induced polarization effects during electronic excitation of the conjugates in the mass spectrometer, since the

Reasonable DFT functionals can be used for smaller molecules (<200 atoms), but investigations of our smallest dimer (1_2^{n+}), excluding the formation of multimers, would already include >300 atoms; hence busting our computational capacities at the moment.^[36]

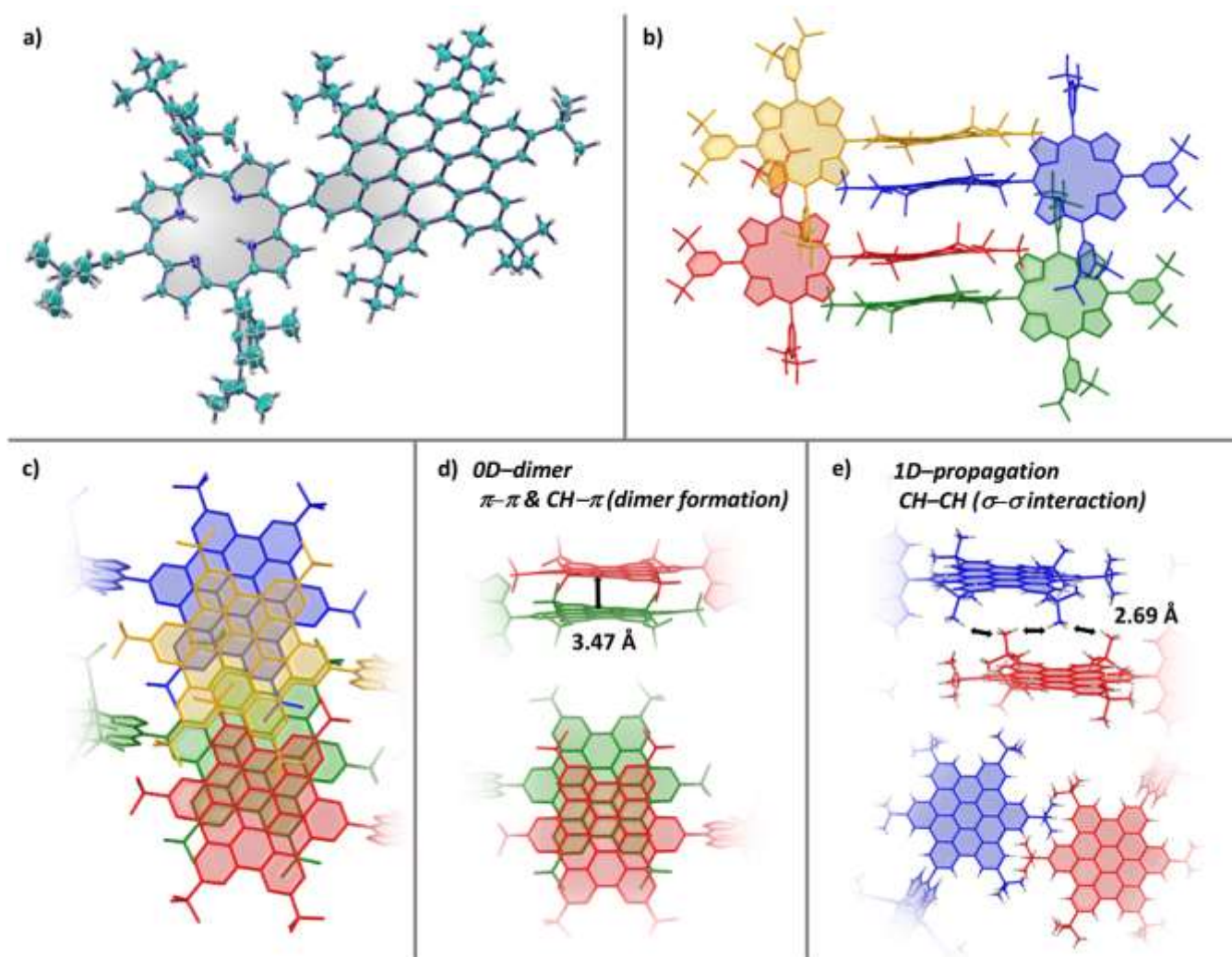


Figure 3. Single crystal structure analysis of **1a**; a) ORTEP model depicted with 50 % thermal ellipsoids; b) side-view on HBC–HBC packing interactions; c) top-view on HBC–HBC packing interactions (from bottom to top: [green]–[red]–[blue]–[orange]); d) zero-dimensional dimer formation between [green] and [red] through π – π and CH– π interactions; e) one-dimensional propagation through CH–CH interactions between [red] and [blue].

We obtained a deeper understanding of the supramolecular binding situation in superbene–porphyrin clusters, by performing XRDA on selected examples. Regrettably, superbene–porphyrins **1**, **2**, **3** and **4** could not be successfully analyzed. However, single crystals suitable for XRDA of **1a** could be obtained by layer diffusion from a toluene/methanol mixture. In the solid state, the HBC plane is tilted by 70° with respect to the porphyrin (compare figure 3a), allowing a reasonable electronic communication between both chromophores. As it can be extracted from figure 3b–3e, two major interaction motifs can be elucidated for **1a**, which can be classified as zero-dimensional interactions and one-dimensional propagation interactions. The 0D–interactions stem from π – π and CH– π interactions of two HBC planes and their *t*Bu groups (compare dimer pairs in figure 3b–d; [green–red] and [blue–orange]). The distance of the respective HBC–dimers is found to be around 3.47 Å, which is in good agreement with the crystal structure analysis of *t*BuHBC (3.44 Å) and which, unlike

n-alkylated HBCs, was found to undergo mere dimer formation in a sandwich–herringbone packing.^[48–50] While a herringbone type packing cannot be observed for **1a**, an attractive one-dimensional CH–CH interaction of the *t*Bu–groups at the periphery of the HBCs with *t*Bu–groups from the next dimer–pair propagates through the crystal (compare figure 3b, c and e; [red–blue]). Hereby, an average H⋯H distance of 2.69 Å can be observed, which is in the perfect range for attractive London dispersion interactions (2.5– 3.0 Å).^[6] In case for Ni^{II}–complex **1aNi**, which shows a saddle–shape distortion of the porphyrin plane, the intermolecular interaction parameters change only marginally to a π – π distance of 3.39 Å for the HBC planes and an averaged H⋯H distance of 2.74 Å for the *t*Bu–groups (see figure S9 in the supporting information). Hence, changing the electronic properties and the shape of the porphyrin by nickel (and zinc as shown for [*trans*HBC]PZn) complexation has no significant impact on the intermolecular interactions, which is

also reflected in the gas-phase cluster formations of **1aNi** versus **1a** (see figure S10 in the supporting information). When it comes to multi-HBC-porphyrin conjugates, these interactions can be imagined to propagate not only in *x*-direction, thus in one dimension, but also into the second- and third-dimensional space. With that said, XRDA of **cis-2a**, which was crystallized by layer diffusion from a mixture of CH₂Cl₂ and methanol, provided an interesting view. As it is depicted in figure 4a, the *cis*-configuration of **cis-2a** leads to the formation of 1D "zig-zag wires". Even though the structure resolution does not

interact with the porphyrin plane of an adjacent molecule via CH- π attractions. However, we believe that these particular interactions are neglectable in the gas phase and are mere findings arising from packing phenomena in the solid state. This assumption is based on the fact that the clustering ability of **1a**, with detected cluster sizes of up to four molecules (see figure S11), and **cis-2a** with clusters of a maximum size of six molecules (figure 4b), are obviously smaller compared to their respective *meso*-H conjugates **1** and **2** and thus the 3,5-di-*t*Bu-phenyl moieties at the porphyrin seem not to contribute to

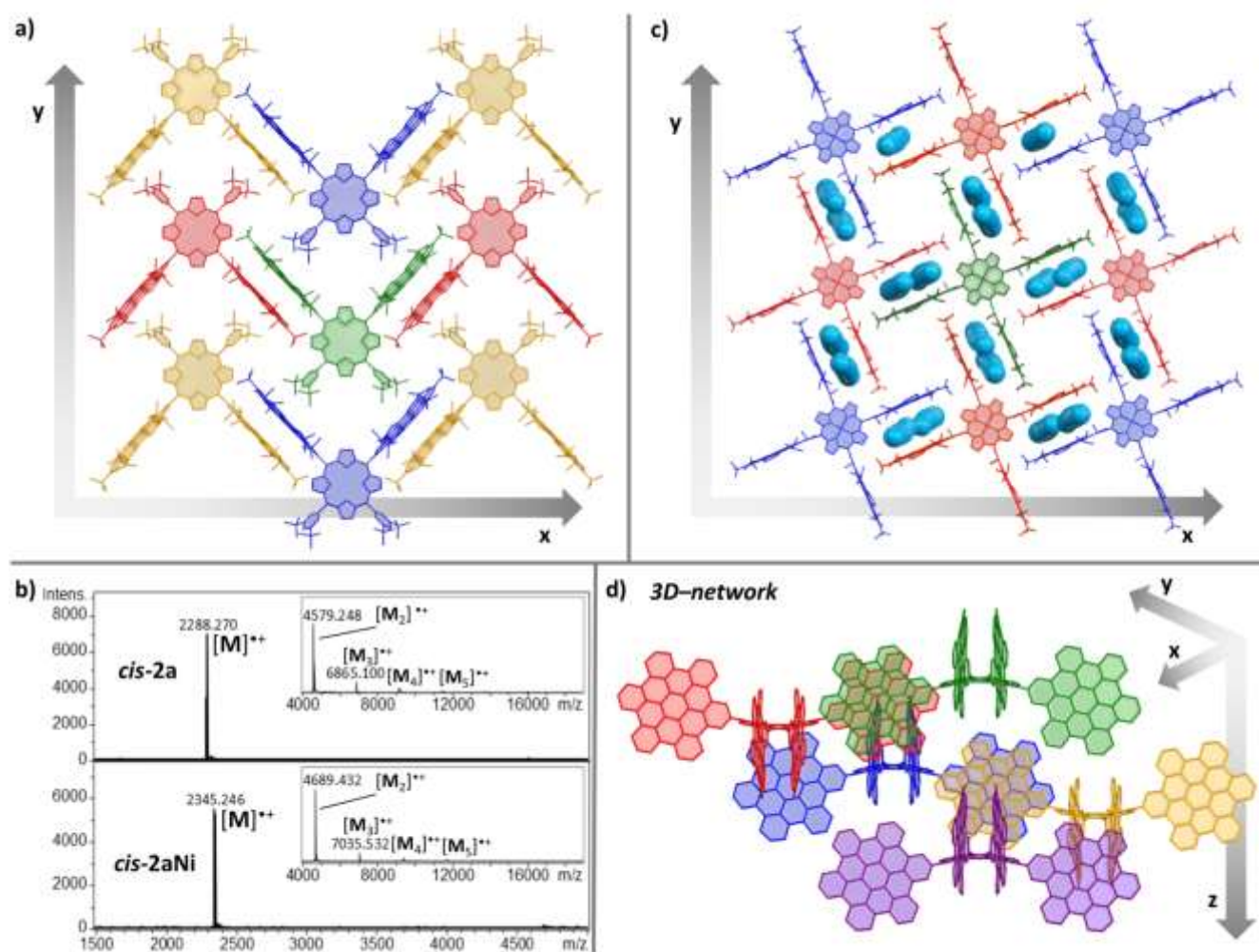


Figure 4. a) Top-view on the two dimensional "carpet-formation" of **cis-2a** through π - π and CH- π interactions; b) MALDI MS of **cis-2a** and the respective nickel-complex **cis-2aNi**; c) top-view on the two-dimensional network of **4Ni**; intercalated *n*-heptane molecules are highlighted in light blue as space filling model structures; d) side-view on the three-dimensional network of **4Ni**; [green] lies directly on top of [purple]; *n*-heptane molecules are omitted for clarity.

allow for detailed assignments of intra- and intermolecular bond lengths, the interactions remind closely of the zero-dimensional interplay, which was discussed above for **1a**. Interestingly, in *y*-direction the next set of zig-zag wire is found to be closely attached via CH- π interactions of the *t*Bu-groups of the aryl moiety at the porphyrin with the HBC plane, forming a "2D-carpet" of linearly assembled zig-zag wires. Similarly, in case of **1a** a few of the *t*Bu-groups of the aryl moiety were found to

attractive interactions. This hypothesis is consistent with the findings of Hwang et al., who demonstrated with their molecular balance model that the nature of the interactions (attractive versus repulsive) of "bulky" *t*Bu-groups are highly dependent on the location at the aryl moiety. Thus, *meta*-positioned *t*Bu-groups in our case did not show attractive interactions, which is also reflected in the high solubility of conjugates **1a** and **cis-2a**.^[8]

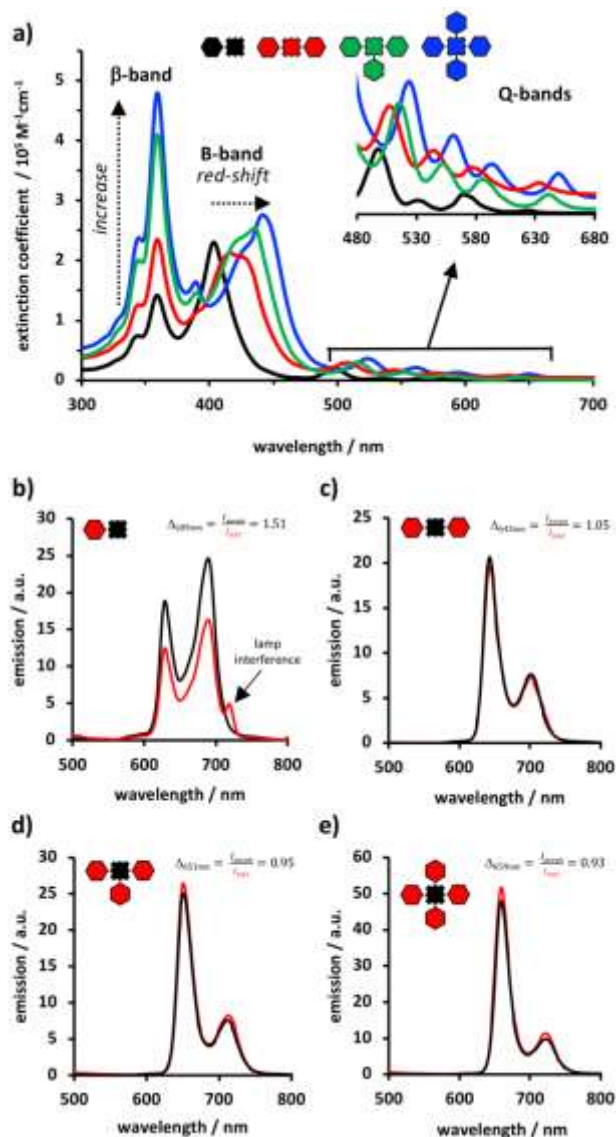


Figure 5. Spectroscopic analysis of HBC-porphyrin conjugates 1–4: a) UV/vis spectra of **1** (black), **2** (red), **3** (green) and **4** (blue) in CH_2Cl_2 at rt; b–e) emission spectra of **1** (b), **2** (c), **3** (d) and **4** (e); excitation of B-band (black) and β -band (red) in CH_2Cl_2 at rt; insert values indicate the ratio of the emission intensity of the porphyrin's Q-bands after excitation of the B-band versus the β -band.

Lastly, a preliminary structure solution of **4Ni**, crystallized from a mixture of CS_2 , CH_2Cl_2 and *n*-heptane shows a consecutive HBC–HBC stacking, as it is true for the OD-dimer of **1a**; though, this time interrupted by intercalated and thus “insulating” *n*-heptane molecules, as it was already observed for the [**transHBC**]P conjugate in 2014.^[37] It was shown that *n*-heptane molecules serve only as “insulators” between the HBC planes, without really affecting the overall packing motif and therefore, they cause a switching between a “conducting” to an “insulating state”. Consequently, upon “virtual-exhaling” of the *n*-heptane molecules, the actual packing pattern in *x*- and *y*-direction becomes readily apparent (see figure 4c). Even more striking

becomes the interaction motif, if the perspective is tilted onto the *z*-axis, hence into the third dimension. Indicated in figure 4d, the molecules interact in such way that the beneath lying layer is interconnected by the respective HBC–HBC interactions, accordingly leading to a dispersion-based 3D-network ([green] molecule is lying directly on top of the [purple] molecule). With this model in hand, the strong cluster formation ability of **3** and **4** becomes reasonable. Despite the sterically much more crowded situation of **3** and **4**, taking into account that all *para*-positions at the HBC are *t*-butylated and the π -surface of the porphyrin plane is not available for any strong interactions, the large clusters in MALDI and the structure analysis conclude that all attractive interactions stem from the $t\text{BuHBC}$ – $t\text{BuHBC}$ interplay. However, the powerful interplay is not solely based on intuitively apparent π – π interactions but appears to benefit largely from σ – π and σ – σ interactions, originating from the peripheral DEDs.

Importantly, the cluster formation ability is not related to the solubility of the molecules in e.g. CH_2Cl_2 or CHCl_3 , which does not only allow the clear analysis by NMR spectroscopy in solution (compare figures S12–S15 in the supporting information), but correlates well to the latest observations by Pollice et al., who found the attenuation of **LD** in CH_2Cl_2 solutions.^[11] A qualitative depiction can be summarized as the following: cluster size: $4 \geq 3 > 2 > 1 \geq 2a > 1a$; solubility (CH_2Cl_2): $1a \geq 2a > 3 \geq 4 > 1 \gg 2$. With that said, one can clearly rule out mere aggregation phenomena due to low solubility, which readily occur in π -rich molecules like e.g., in unsubstituted HBC–porphyrin conjugates,^[37] or large polycyclic aromatic hydrocarbons. In fact, some of the HPB-porphyrin conjugates like e.g., 5,15-bis-HPB-porphyrin (precursor of **2**), show to be almost insoluble in common solvents like e.g., CH_2Cl_2 , but no evidence for cluster formation in MALDI could be detected.

Finally, the absorption and emission properties of conjugates **1**–**4**, shown in figure 5, are discussed. As depicted in figure 5a, the absorption characteristics of the HBC-moieties remain, besides an increased extinction coefficient upon increasing the number of HBCs in the conjugate, unchanged; no shift of the β -bands (358 nm) are observed. On the other hand, the porphyrins B- and Q-bands exhibit distinct red shifts, with absorption maxima for the B-band at 402 (**1**), 415 (**2**), 434 (**3**) and 441 nm (**4**). Furthermore, a remarkable broadening of the B-band with rising number of HBCs is observed. Additionally, conjugates **2**, **3** and **4** show a split in the B-band. Upon excitation of the conjugates, a very efficient energy transfer from the HBC-periphery to the porphyrin core can be observed (figure 5b–e). Excitation of the β -band leads exclusively to the emission of the porphyrins Q-band and no emission from the HBC moieties can be observed in any of the conjugates. While the ratio of emission intensity for **1** is higher upon excitation of the porphyrin itself, conjugates **2**, **3** and **4** show ratios close to one, underpinning the efficient energy transfer. In fact, conjugates **3** and **4** show slightly higher porphyrin Q-band emissions after excitation of the HBC's β -band, than after the B-band.

Conclusions

In summary, we presented our comprehensive study on **superbenzene**-porphyrin conjugates. The majority of conjugates could be synthesized by a microwave-assisted condensation protocol utilizing *tert*-butylated hexaphenylbenzene aldehyde (**HPB-CHO**), followed by Scholl oxidation. By performing MALDI mass spectrometric experiments, we showed that superbenzene-porphyrin conjugates undergo supramolecular cluster formations. These clusters can be detected in the gas phase, with their size depending on the number of *t*BuHBCs in the periphery of the porphyrin. The clusters can grow at least to twenty molecules, which are held together by attractive London dispersion interactions (π - π , σ - π and σ - σ) that spread into all three dimensions. By ESI-CID experiments with dimers of **TPP**, **tBuHBC** and the composite of **TPP/tBuHBC**, the origin of the attractive interactions could be identified to stem from the *t*BuHBCs. XRDA of free-base and metalated conjugates came to the same conclusion in the solid state, if no "insulators" like *n*-heptane were present. Importantly, the cluster formation ability shows no correlation to the solubility of the conjugates, which is in agreement with the attenuation of London dispersion in CH₂Cl₂ solutions. By variation of the amount of used matrix, we come to the conclusion that the clusters observed in MALDI are likely pre-formed during the sample preparation process, which are then transported into the gas phase upon ionization. By absorption and emission spectroscopy, we revealed an efficient energy transfer from the HBC-periphery to the porphyrin. At that stage, we believe that during the excitation/ionization process the cluster formation is enhanced due to the occupation of higher lying orbitals of the conjugates, subsequently leading to increased polarizabilities and thus enhanced dispersion interactions. However, this hypothesis is currently under investigation. In regards to above discussions, self-assembled molecular tectonics based on functional molecules, like in our case porphyrins and HBCs, are imaginable to serve for numerous applications, spread from e.g., catalysis to electronics. Importantly, the architectures are not based on covalent bonds; thus, the nature of the van der Waals interactions allows for dynamic transformations and adaptations to their environment. With our findings, we believe that we enlarge the view on design strategies of self-assembled materials that incorporate DEDs as directing units, but still remain easily processable in solution.

Acknowledgements

We are grateful for the financial support from the German Research Council (DFG SFB 953 – "Synthetic Carbon Allotropes", Project A2 and Z1). DL and JFH thank the Graduate School of Molecular Science (GSMS) for financial support. DL thanks the Alexander von Humboldt foundation and the Japan Society for the Promotion of Science (JSPS) for a fellowship.

Keywords: Porphyrin • Hexabenzocoronene • Cluster • Mass spectrometry • Dispersion Interaction

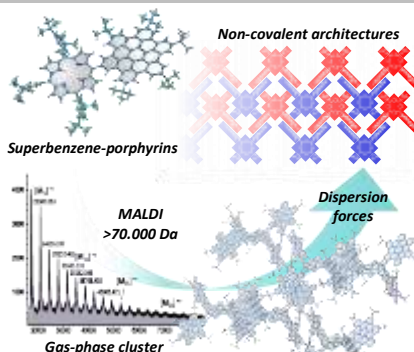
- ‡ Results are taken in parts from: D. Lungerich, Doctoral Thesis, Friedrich-Alexander-Universität Erlangen-Nürnberg, 2017.
- [1] K.-T. Tang, J. P. Toennies, *Angew. Chem. Int. Ed.* **2010**, *122*, 9574–9579; *Angew. Chem.* **2010**, *122*, 9768–9774.
- [2] J. P. Wagner, P. R. Schreiner, *Angew. Chem. Int. Ed.* **2015**, *54*, 12274–12296; *Angew. Chem.* **2015**, *127*, 12446–12471.
- [3] P. R. Schreiner, L. V. Chernish, P. A. Gunchenko, E. Y. Tikhonchuk, H. Hausmann, M. Serafin, S. Schlecht, J. E. P. Dahl, R. M. K. Carlson, A. A. Fokin, *Nature* **2011**, *477*, 308–311.
- [4] S. Grimme, R. Huenerbein, S. Ehrlich, *ChemPhysChem* **2011**, *12*, 1258–1261.
- [5] S. Grimme, P. R. Schreiner, *Angew. Chem. Int. Ed.* **2011**, *50*, 12639–12642; *Angew. Chem.* **2011**, *123*, 12849–12853.
- [6] J. P. Wagner, P. R. Schreiner, *J. Chem. Theory Comput.* **2014**, *10*, 1353–1358.
- [7] J. P. Wagner, P. R. Schreiner, *J. Chem. Theory Comput.* **2016**, *12*, 231–237.
- [8] J. Hwang, P. Li, M. D. Smith, K. D. Shimizu, *Angew. Chem. Int. Ed.* **2016**, *55*, 8086–8089; *Angew. Chem.* **2016**, *128*, 8218–8221.
- [9] S. Rösel, H. Quanz, C. Logemann, J. Becker, E. Mossou, L. Canadillas-Delgado, E. Caldeweyher, S. Grimme, P. R. Schreiner, *J. Am. Chem. Soc.* **2017**, *139*, 7428–7431.
- [10] S. Rösel, C. Balestrieri, P. R. Schreiner, *Chem. Sci.* **2017**, *8*, 405–410.
- [11] R. Pollice, M. Bot, I. J. Kobylanski, I. Shenderovich, P. Chen, *J. Am. Chem. Soc.* **2017**, *139*, 13126–13140.
- [12] F. London, *Z. Phys.* **1930**, *63*, 245–279.
- [13] F. London, *Trans. Faraday Soc.* **1937**, *33*, 8–26.
- [14] B. Kohl, M. V. Bohnwagner, F. Rominger, H. Wadeppohl, A. Dreuw, *Mastalerz, Chem. Eur. J.* **2015**, *22*, 646–655.
- [15] K. Shibasaki, A. Fujii, N. Mikami, S. Tsuzuki, *J. Phys. Chem. A* **2006**, *110*, 4397–4404.
- [16] M. Busker, T. Häber, M. Nispel, K. Kleinermanns, *Angew. Chem. Int. Ed.* **2008**, *47*, 10094–10097; *Angew. Chem.* **2008**, *120*, 10248–10251.
- [17] A. Fujii, H. Hayashi, J. W. Park, T. Kazama, N. Mikami, S. Tsuzuki, *Phys. Chem. Chem. Phys.* **2011**, *13*, 14131–14141.
- [18] C. Tyborski, R. Meinke, R. Gillen, T. Bischoff, A. Knecht, R. Richter, A. Merli, A. A. Fokin, T. V. Koso, V. N. Rodionov, et al., *J. Chem. Phys.* **2017**, *147*, 044303.
- [19] I. K. Mati, S. L. Cockroft, *Chem. Soc. Rev.* **2010**, *39*, 4195–4205.
- [20] W. R. Carroll, P. Pellechia, K. D. Shimizu, *Org. Lett.* **2008**, *10*, 3547–3550.
- [21] W. R. Carroll, C. Zhao, M. D. Smith, P. J. Pellechia, K. D. Shimizu, *Org. Lett.* **2011**, *13*, 4320–4323.
- [22] A. Nijamudheen, D. Jose, A. Shine, A. Datta, *J. Phys. Chem. Lett.* **2012**, *3*, 1493–1496.
- [23] L. Yang, C. Adam, G. S. Nichol, S. L. Cockroft, *Nat. Chem.* **2013**, *5*, 1006–1010.
- [24] C. Adam, L. Yang, S. L. Cockroft, *Angew. Chem. Int. Ed.* **2015**, *54*, 1164–1167; *Angew. Chem.* **2015**, *127*, 1180–1183.
- [25] B. Bhayana, C. S. Wilcox, *Angew. Chem. Int. Ed.* **2007**, *46*, 6833–6836; *Angew. Chem.* **2007**, *119*, 6957–6960.
- [26] L. Yang, J. B. Brazier, T. A. Hubbard, D. M. Rogers, S. L. Cockroft, *Angew. Chem. Int. Ed.* **2016**, *55*, 912–916; *Angew. Chem.* **2016**, *128*, 924–928.
- [27] D. J. Pascoe, K. B. Ling, S. L. Cockroft, *J. Am. Chem. Soc.* **2017**, *139*, 15160–15167.
- [28] S. Grimme, A. Hansen, J. G. Brandenburg, C. Bannwarth, *Chem. Rev.* **2016**, *116*, 5105–5154.
- [29] L. Goerigk, S. Grimme, *Phys. Chem. Chem. Phys.* **2011**, *13*, 6670–6688.
- [30] C. R. Martinez, B. L. Iverson, *Chem. Sci.* **2012**, *3*, 2191–2201.
- [31] S. Grimme, J.-P. Djukic, *Inorg. Chem.* **2011**, *50*, 2619–2628.
- [32] S. O. Nilsson Lill, P. Ryberg, T. Rein, E. Bennström, P. O. Norrby, *Chem. Eur. J.* **2012**, *18*, 1640–1649.

- [33] H. Arp, J. Baumgartner, C. Marschner, P. Zark, T. Müller, *J. Am. Chem. Soc.* **2012**, *134*, 6409–6415.
- [34] L. Schweighauser, M. A. Strauss, S. Bellotto, H. A. Wegner, *Angew. Chem. Int. Ed.* **2015**, *54*, 13436–13439; *Angew. Chem.* **2015**, *127*, 13636–13639.
- [35] S. Grimme, in *The Chemical Bond. Fundamental Aspects of Chemical Bonding*. (Ed. G. Frenking, S. Shaik), Wiley-VCH, Weinheim, **2014**, p. 477.
- [36] J. Hermann, R. A. DiStasio Jr., A. Tkatchenko, *Chem. Rev.* **2017**, *117*, 4714–4758.
- [37] J. M. Englert, J. Malig, V. A. Zamolo, H. Andreas, N. Jux, *Chem. Commun.* **2013**, *49*, 4827–4829.
- [38] D. Lungerich, J. F. Hitznerberger, M. Marcia, F. Hampel, T. Drewello, N. Jux, *Angew. Chem. Int. Ed.* **2014**, *53*, 12231–12235; *Angew. Chem.* **2014**, *126*, 12427–12431.
- [39] D. Lungerich, J. F. Hitznerberger, W. Donaubaue, T. Drewello, N. Jux, *Chem. Eur. J.* **2016**, *22*, 16755–16759.
- [40] M. M. Martin, N. Jux, *J. Porphyrins Phthalocyanines* **2018**, *22*, 454–460.
- [41] J. S. Lindsey, I. C. Schreiman, H. C. Hsu, P. C. Kearney, A. M. Marguerettaz, *J. Org. Chem.* **1987**, *52*, 827–836.
- [42] A. Wiehe, C. Ryppa, M. O. Senge, *Org. Lett.* **2002**, *4*, 3807–3809.
- [43] R. Lucas, J. Vergnaud, K. Teste, R. Zerrouki, V. Sol, P. Krausz, *Tetrahedron Lett.* **2008**, *49*, 5537–5539.
- [44] B. Boens, P.-A. Faugeras, J. Vergnaud, R. Lucas, K. Teste, R. Zerrouki, *Tetrahedron* **2010**, *66*, 1994–1996.
- [45] H. Mori, T. Tanaka, A. Osuka, *J. Mater. Chem. C* **2013**, *1*, 2500–2519.
- [46] G. E. Ewing, *Angew. Chem. Int. Ed.* **1972**, *11*, 486–495; *Angew. Chem.* **2072**, *84*, 570–580.
- [47] J. Hermann, D. Alfé, A. Tkatchenko, *Nat. Commun.* **2017**, *8*, 14052–14059.
- [48] P. Herwig, V. Enkelmann, O. Schmelz, K. Müllen, *Chem. Eur. J.* **2000**, *6*, 1834–1839.
- [49] S. Ito, M. Wehmeier, J. D. Brand, C. Kübel, R. Epsch, J. P. Rabe, K. Müllen, *Chem. Eur. J.* **2000**, *6*, 4327–4342.
- [50] M. Kastler, W. Pisula, D. Wasserfallen, T. Pakula, K. Müllen, *J. Am. Chem. Soc.* **2005**, *127*, 4286–4296.

Entry for the Table of Contents (Please choose one layout)

FULL PAPER

Superbenzene-porphyrin conjugates were synthesized that show a high cluster formation ability. The cluster size correlates to the amount of *tert*-butylated hexa-*peri*-hexabenzocoronenes attached to the porphyrin's periphery. Determined by mass spectrometry and X-ray diffraction, London dispersion interactions stemming from the *tert*-butyl groups were identified to be the major reason for the cluster formation.



D. Lungerich, J. F. Hitzenberger, F. Hampel, T. Drewello, N. Jux**

Page No. – Page No.

Superbenzene–Porphyrin Gas-Phase Architectures Derived from Intermolecular Dispersion Interactions